

Production of a_0 -mesons in pp and pn reactions ‡

E.L. Bratkovskaya †, V. Yu. Grishina ‖§, L.A. Kondratyuk ‡⁺,
M. Büscher ⁺ and W. Cassing †

†Institut für Theoretische Physik, Universität Giessen, D-35392 Giessen, Germany

‖ Institute for Nuclear Research, 60th October Anniversary Prospect 7A, 117312
Moscow, Russia

§Institute of Theoretical and Experimental Physics, B.Chermushkinskaya 25, 117259
Moscow, Russia

⁺ Institut für Kernphysik, Forschungszentrum Jülich, D-52425 Jülich, Germany

Abstract. We investigate the cross section for the reaction $NN \rightarrow NN a_0$ near threshold and at medium energies. An effective Lagrangian approach with one-pion exchange is applied to analyze different contributions to the cross section for different isospin channels. The Reggeon exchange mechanism is also considered. The results are used to calculate the contribution of the a_0 meson to the cross sections and invariant $K\bar{K}$ mass distributions of the reactions $pp \rightarrow pnK^+\bar{K}^0$ and $pp \rightarrow ppK^+K^-$. It is found that the experimental observation of a_0^+ mesons in the reaction $pp \rightarrow pnK^+\bar{K}^0$ is much more promising than the observation of a_0^0 mesons in the reaction $pp \rightarrow ppK^+K^-$.

PACS: 25.10.+s, Meson production and 13.75.-n, Proton induced reactions

Submitted to: *J. Phys. G: Nucl. Phys.*

1. Introduction

The excitations of the QCD vacuum with different quantum numbers as well as their life times and decay modes are of fundamental interest in the physics of the strong interaction. The masses of the pseudo-scalar mesons have been found to be essentially due to a spontaneous breaking of the chiral $SU(3)_R \times SU(3)_L$ symmetry or the $U(1)_A$ anomaly (in case of the η'). The vector mesons ρ , ω , ϕ , K^* , J/Ψ etc., which are the dipole modes of the vacuum, have found increasing attention during the last two decades. Especially their decay to dileptons is presently investigated in elementary and complex (nucleus-nucleus) collisions in different laboratories all over the world (cf. the reviews [1, 2, 3] and Refs. therein). On the other hand, the scalar sector of vacuum excitations is not well known experimentally and theoretically, so far.

The structure of the lightest scalar mesons $a_0(980)$ and $f_0(980)$ is still under discussion (see e.g. [4, 5, 6, 7, 8, 9, 10] and references therein). Different authors interpreted them as unitarized $q\bar{q}$ states or as four-quark cryptoexotic states or as $K\bar{K}$ molecules or even as vacuum scalars (Gribov's minions). Although it has been possible to describe them as ordinary $q\bar{q}$ -states (see Refs. [11, 12, 13]), other options cannot be ruled out up to now. Another problem is the possible strong mixing between the uncharged $a_0(980)$ and the $f_0(980)$ due to a common coupling to $K\bar{K}$ intermediate states [14, 15, 16, 17],[18, 19, 20]. This effect can influence the structure of the uncharged component of the $a_0(980)$ and implies that it is important to perform a comparative study of a_0^0 and a_0^+ (or a_0^-). There is no doubt that new data on a_0^0 and a_0^+/a_0^- production in πN and NN reactions are quite important to shed new light on the a_0 structure and the dynamics of its production.

In our recent paper [21] we have considered a_0 production in the reaction $\pi N \rightarrow a_0 N$ near the threshold and at GeV energies. An effective Lagrangian approach as well as the Regge pole model were applied to investigate different contributions to the cross-section of the reaction $\pi N \rightarrow a_0 N$. Here we employ the latter results for an analysis of a_0 production in NN collisions. Our study is particularly relevant to the current experimental program at COSY-Jülich [22, 23, 24].

Our paper is organized as follows: In Sect. 2 we discuss an effective Lagrangian approach with one-pion exchange while the Reggeon exchange model is considered in Sect. 3. Sect. 4 is devoted to the calculations of the cross section for the reaction $NN \rightarrow NN a_0$. In Sect. 5 we analyze the contribution of the a_0 resonance to the cross sections and invariant $K\bar{K}$ mass distributions for the reactions $pp \rightarrow pp K^+ K^-$ and $pp \rightarrow pn K^+ \bar{K}^0$. Our conclusions are presented in Sect. 6.

2. An effective Lagrangian approach with one-pion exchange

We consider a_0^0 , a_0^+ , a_0^- production in the reactions $j = pp \rightarrow ppa_0^0$, $pp \rightarrow pna_0^+$, $pn \rightarrow ppa_0^-$ and $pn \rightarrow pna_0^0$ using the effective Lagrangian approach with one-pion exchange (OPE). For the elementary $\pi N \rightarrow Na_0$ transition amplitude we take into

account different mechanisms α corresponding to t -channel diagrams with $\eta(550)$ - and $f_1(1285)$ -meson exchanges ($\alpha = t(\eta), t(f_1)$) as well as s - and u -channel graphs with an intermediate nucleon ($\alpha = s(N), u(N)$) (cf. Ref. [21]). The corresponding diagrams are shown in Fig. 1. The invariant amplitude of the $NN \rightarrow NN a_0$ reaction then is the sum of the four basic terms (diagrams in Fig. 1) with permutations of nucleons in the initial and final states

$$\begin{aligned} \mathcal{M}_{j(\alpha)}^\pi[ab; cd] &= \xi_{j(\alpha)}^\pi[ab; cd] \mathcal{M}_\alpha^\pi[ab; cd] + \xi_{j(\alpha)}^\pi[ab; dc] \mathcal{M}_\alpha^\pi[ab; dc] \\ &+ \xi_{j(\alpha)}^\pi[ba; dc] \mathcal{M}_\alpha^\pi[ba; dc] + \xi_{j(\alpha)}^\pi[ba; cd] \mathcal{M}_\alpha^\pi[ba; cd], \end{aligned} \quad (1)$$

where the coefficients $\xi_{j(\alpha)}^\pi$ are given in Table 1. The amplitude for the t -channel exchange with $\eta(550)$ - and $f_1(1285)$ -mesons are given by

$$\begin{aligned} \mathcal{M}_{t(\eta)}^\pi[ab; cd] &= g_{a_0\eta\pi} F_{a_0\eta\pi} \left((p_a - p_c)^2, (p_d - p_b)^2 \right) g_{\eta NN} F_\eta \left((p_a - p_c)^2 \right) \\ &\times \frac{1}{(p_a - p_c)^2 - m_\eta^2} \bar{u}(p_c) \gamma_5 u(p_a) \times \Pi(p_b; p_d), \end{aligned} \quad (2)$$

$$\begin{aligned} \mathcal{M}_{t(f_1)}^\pi[ab; cd] &= -g_{a_0 f_1 \pi} F_{a_0 f_1 \pi} \left((p_a - p_c)^2, (p_d - p_b)^2 \right) g_{f_1 NN} F_{f_1} \left((p_a - p_c)^2 \right) \\ &\times \frac{1}{(p_a - p_c)^2 - m_{f_1}^2} (p_a - p_c + 2(p_b - p_d))_\mu \left(g_{\mu\nu} - \frac{(p_a - p_c)_\mu (p_a - p_c)_\nu}{m_{f_1}^2} \right) \\ &\times \bar{u}(p_c) \gamma_5 \gamma_\nu u(p_a) \times \Pi(p_b; p_d), \end{aligned} \quad (3)$$

with

$$\Pi(p_b; p_d) = \frac{f_{\pi NN}}{m_\pi} F_\pi \left((p_b - p_d)^2 \right) (p_b - p_d)_\beta \bar{u}(p_d) \gamma_5 \gamma_\beta u(p_b) \frac{1}{(p_b - p_d)^2 - m_\pi^2}. \quad (4)$$

The amplitudes for the s - and u -channels (lower part of Fig. 1) are given as

$$\begin{aligned} \mathcal{M}_{s(N)}^\pi[ab; cd] &= \Pi(p_b; p_d) \frac{f_{\pi NN}}{m_\pi} F_\pi \left((p_d - p_b)^2 \right) g_{a_0 NN} \frac{F_N \left((p_a + p_b - p_d)^2 \right)}{(p_a + p_b - p_d)^2 - m_N^2} \\ &\times (p_d - p_b)_\mu \bar{u}(p_c) [(p_a + p_b - p_d)_\delta \gamma_\delta + m_N] \gamma_5 \gamma_\mu u(p_a), \end{aligned} \quad (5)$$

$$\begin{aligned} \mathcal{M}_{u(N)}^\pi[ab; cd] &= \Pi(p_b; p_d) \frac{f_{\pi NN}}{m_\pi} F_\pi \left((p_d - p_b)^2 \right) g_{a_0 NN} \frac{F_N \left((p_c + p_d - p_b)^2 \right)}{(p_c + p_d - p_b)^2 - m_N^2} \\ &\times (p_d - p_b)_\mu \bar{u}(p_c) \gamma_5 \gamma_\mu [(p_c + p_d - p_b)_\delta \gamma_\delta + m_N] u(p_a). \end{aligned} \quad (6)$$

Here p_a, p_b and p_c, p_d are the four momenta of the initial and final nucleons, respectively.

The effective Lagrangians involving a_0 and f_1 mesons were taken in the following forms:

$$\begin{aligned} \mathcal{L}_{a_0\eta\pi} &= g_{a_0\eta\pi} \eta(x) \pi(x) a_0(x), \\ \mathcal{L}_{a_0 f_1 \pi} &= g_{a_0 f_1 \pi} \epsilon_\lambda^{f_1}(x) \partial^\lambda \pi(x) a_0(x), \\ \mathcal{L}_{a_0 NN} &= g_{a_0 NN} \bar{\Psi}_N(x) a_0(x) \Psi_N(x), \\ \mathcal{L}_{f_1 NN} &= g_{f_1 NN} \epsilon_\lambda^{f_1}(x) \bar{\Psi}_N(x) \gamma^\lambda \Psi_N(x). \end{aligned} \quad (7)$$

We mostly employ coupling constants and form factors from the Bonn-Jülich potentials (see e.g. Refs. [25, 26, 27]).

The functions F_i in Eqs. (2)-(6) represent form factors for virtual mesons at the different vertices i ($i = \pi, \eta, f_1$) and for each vertex they are taken in the monopole form

$$F_i(t) = \frac{\Lambda_i^2 - m_i^2}{\Lambda_i^2 - t}, \quad (8)$$

where Λ_i is a cut-off parameter. For the 'effective' π exchange we use the coupling constant $f_{\pi NN}^2/4\pi = 0.08$ and cut-off parameter $\Lambda_{\pi NN} = 1.05 \div 1.3$ GeV. In the case of η exchange we take $g_{\eta NN}^2/4\pi = 3$, $\Lambda_{\eta NN} = 1.5$ GeV and $g_{a_0\eta\pi} = 2.46$ GeV, which results from the width $\Gamma(a_0 \rightarrow \eta\pi) = 80$ MeV.

The contribution of the f_1 exchange is calculated with $g_{f_1 NN} = 11.2$, $\Lambda_{f_1 NN} = 1.5$ GeV from Ref. [27] and $g_{a_0 f_1 \pi} = 2.5$. The latter value for $g_{a_0 f_1 \pi}$ corresponds to $\Gamma_{tot}(f_1) = 24$ MeV and $Br(f_1 \rightarrow a_0\pi) = 34\%$. The same parameters have been used in our previous study of a_0 production in $\pi N \rightarrow a_0 N$ and $pp \rightarrow da_0^+$ reactions [21].

For the form factors at the $a_0 f_1 \pi$ (as well as $a_0 \eta \pi$) vertex factorized forms are applied following the assumption from Refs. [28, 29],

$$F_{a_0 f_1 \pi}(t_1, t_2) = F_{f_1 NN}(t_1) F_{\pi NN}(t_2), \quad (9)$$

where $F_{f_1 NN}(t)$, $F_{\pi NN}(t)$ are taken as in (8).

According to different versions of the Bonn potential the coupling constant $g_{a_0 NN}^2/4\pi$ can vary from 1.1075 to 2.67 [25, 27]. On the other hand, the unitary model for meson-nucleon scattering [30] gives a different range for this constant from 0.0026 to 0.88. In the latter model the a_0 only gives a contribution to the $\pi\eta$ background because there are no known resonances which decay to $a_0 N$. Since the model is extended only up to energies $\sqrt{s} \leq 1.9$ GeV, which is below the a_0 threshold, the meson-nucleon dynamics is not very sensitive to the $a_0 NN$ coupling. We note that a small value of $g_{a_0 NN}^2/4\pi$ certainly contradicts the experimental values of $Br(p\bar{p} \rightarrow a_0\pi) = 0.69 \pm 0.12$ [31] and $Br(p\bar{p} \rightarrow a_0\omega) = 0.354 \pm 0.028$ [32], which are quite large (see e.g. Refs. [26, 27]). Having in mind these considerations we take (as well as in Ref. [21]) the minimal value suggested by the Bonn potential $g_{a_0 NN} \simeq 3.7$. This value is not very different from the upper value of 3.33 given by the model of Ref. [30].

Another problem is the treatment of a virtual nucleon. In this case – instead of the product of two monopole form factors (at the $a_0 NN$ and πNN vertices) – we use a dipole-like form factor,

$$F_N(s) = \frac{\Lambda_N^4}{\Lambda_N^4 + (s - m_N^2)^2}, \quad (10)$$

which is normalized at $s = m^2$ and has the same asymptotics at large s (positive or negative) as $F_i(s)F_j(s)$.

There are a couple of arguments in favour of using the form factor (10) for virtual nucleons instead of those which are applied for virtual mesons. In the t -channel graph in elastic NN scattering the value of t is negative and the monopole form factor F_π as given by Eq. (8) does not have a singularity in the physical region and decreases with t . For the s -channel graph with a nucleon exchange in the $\pi N \rightarrow a_0 N$ amplitude the

value of s is positive in the physical region and the conventional form factor

$$\frac{\Lambda_N^2 - m_N^2}{\Lambda_N^2 - s}$$

may have even a pole in the physical region (this happens for $\Lambda_N = 2$ GeV, which is used in the Bonn potential for a virtual a_0). This undesirable property is absent in the form factor (10), where we consider the cut-off Λ_N as a free parameter. In our previous work [21] we fixed Λ_N in the interval 1.2-1.3 GeV using experimental data on the differential cross section of the reaction $pp \rightarrow da_0^+$ at $p_{lab} = 3.8 \div 6.3$ GeV/ c [33]; in this study we take $\Lambda_N = 1.24$ GeV as an average value (see also the discussion in Section 4).

We recall that the functional form of the nucleon form factor given by (10) was used in many papers, where meson production in πN , γN and NN collisions has been discussed (see e.g. [29, 30, 34, 35, 36, 37] and references therein).

The total cross section for a_0 production in the isospin reaction j is given as the coherent sum of the amplitudes (1) over all channels ($\alpha = s(N), u(N), t(f_1), t(\eta)$) integrated over phase space

$$\sigma_{a_0}^j(s) = \int dE_c dq_0 d\cos\theta_q d\varphi_q \frac{1}{2^9 \pi^4 p_a \sqrt{s}} \left| \sum_{\alpha} \mathcal{M}_{j(\alpha)}^{\pi}[ab; cd] \right|^2. \quad (11)$$

Here $s = (p_a + p_b)^2$ is the total energy of the NN system squared, E_c and q_0 are the energy of the outgoing nucleon and a_0 meson, respectively. θ_q is the polar angle of the 3-momentum of the a_0 -meson \mathbf{q} in the cms of the initial nucleons defined as $\theta_q = \mathbf{q}, \widehat{\mathbf{p}}_{\mathbf{a}}$, while φ_q is the azimuthal angle of \mathbf{q} in the cms.

As shown in the analysis in Ref. [21] the contribution of the η -exchange to the amplitude $\pi N \rightarrow a_0 N$ is small. Note that in Ref. [38] only this mechanism was taken into account for the reaction $pn \rightarrow ppa_0^-$. Here we also include the η -exchange because it might be noticeable in those isospin channels where a strong destructive interference of u - and s -channel terms can occur (see below).

3. The Reggeon exchange model

Here as in Ref. [21] we also use the Regge-pole model for the amplitude $\pi N \rightarrow a_0 N$ as developed by Achasov and Shestakov [15]. The s -channel helicity amplitudes for the reaction $\pi^- p \rightarrow a_0^0 n$ in this approach can be written as

$$M_{\lambda_2 \lambda_2}(\pi^- p \rightarrow a_0^0 n) = \bar{u}_{\lambda_2}(p_2) \left[-A(s, t) + (p_1 + p_1')_{\alpha} \gamma_{\alpha} \frac{B(s, t)}{2} \right] \gamma_5 u_{\lambda_2}(p_1) \quad (12)$$

where the invariant amplitudes $A(s, t)$ and $B(s, t)$ do not contain kinematical singularities. The relations between the invariant and s -wave helicity amplitudes are given by

$$M_{++} = -M_{--} = \cos \frac{\theta}{2} \left[A(s, t) \sqrt{-t_{min}} - B(s, t) \sqrt{-t_{max} s} \right], \quad (13)$$

$$M_{+-} = M_{-+} = \cos \frac{\theta}{2} \left[A(s, t) \sqrt{-t_{max}} - B(s, t) \sqrt{-t_{min} s} \right], \quad (14)$$

where θ is the c.m. scattering angle, while t_{min} and t_{max} are the values of t at $\theta=0^\circ$ and 180° , respectively.

In the model of Ref. [15] the s -channel helicity amplitudes are expressed through the b_1 and the conspiring ρ_2 Regge trajectories exchange as follows

$$M_{++} = \gamma_{\rho_2}(t) \exp \left[-i \frac{\pi}{2} \alpha_{\rho_2}(t) \right] \left(\frac{s}{s_0} \right)^{\alpha_{\rho_2}(t)}, \quad (15)$$

$$M_{+-} = \sqrt{(t_{min} - t)/s_0} \gamma_{b_1}(t) i \exp \left[-i \frac{\pi}{2} \alpha_{b_1}(t) \right] \left(\frac{s}{s_0} \right)^{\alpha_{b_1}(t)}. \quad (16)$$

As in Ref. [21] we take the meson Regge trajectories in linear form $\alpha_j(t) = \alpha_j(0) + \alpha'_j(0)t$ with $\alpha_{b_1}(0) \simeq -0.37$, $\alpha_{\rho_2}(0) \simeq -0.6$ and $\alpha'_{b_1}(0) = \alpha'_{\rho_2}(0) = 0.9 \text{ GeV}^{-2}$. The residues are parametrized in a conventional way, $\gamma_{\rho_2}(t) = \gamma_{\rho_2}(0) \exp(b_{\rho_2}t)$, $\gamma_{b_1}(t) = \gamma_{b_1}(0) \exp(b_{b_1}t)$; all parameters were taken the same as in Ref. [21]. They correspond to two fits of the Brookhaven data on $d\sigma/dt$ at 18 GeV/c [39] found by Achasov and Shestakov [15]: a) with pure ρ_2 contribution and b) with combined $\rho_2 + b_1$ contribution.

The invariant amplitude corresponding to the diagram of Fig. 2 can be written as

$$\begin{aligned} \mathcal{M}_{Regge}^\pi[ab; cd] &= \bar{u}(p_c) \left[-A(s, t) + (p_{a_0} + p_d - p_b)_\alpha \gamma_\alpha \frac{B(s, t)}{2} \right] \gamma_5 u(p_a) \\ &\times \bar{u}(p_d) \gamma_5 u(p_b) \times \Pi(p_b; p_d). \end{aligned} \quad (17)$$

4. The reaction $NN \rightarrow NN a_0$

In order to demonstrate the sensitivity of the effective OPE model to the cut-off parameter $\Lambda_{\pi NN}$ used in the πNN vertices we show in Fig. 3 the total cross section for the reaction $pp \rightarrow pna_0^+$ for $u(N)$ and $t(f_1)$ channels as a function of the excess energy $Q = \sqrt{s} - \sqrt{s_0}$, where $\sqrt{s_0} = m_{a_0} + 2m_N$, calculated for different cut-off parameters. The dotted lines correspond to $\Lambda_{\pi NN} = 0.8 \text{ GeV}$, the solid lines show the result for $\Lambda_{\pi NN} = 1.05 \text{ GeV}$ whereas the dashed lines indicate $\Lambda_{\pi NN} = 1.3 \text{ GeV}$. The results for $\Lambda_{\pi NN} = 1.3 \text{ GeV}$ and 0.8 GeV differ by a factor of ~ 5 . For our subsequent calculation we choose $\Lambda_{\pi NN} = 1.05 \text{ GeV}$ while keeping the uncertainty on $\Lambda_{\pi NN}$ in our 'effective' approach in mind.

Since we have two nucleons in the final state it is necessary to take into account their final-state-interaction (FSI), which has some influence on meson production near threshold. For this purpose we adopt the FSI model from Ref. [40] based on the (realistic) Paris potential. We use, however, the enhancement factor $F_{NN}(q_{NN})$ – as given by this model – only in the region of small relative momenta of the final nucleons $q_{NN} \leq q_0$, where it is larger than 1. Having in mind that this factor is rather uncertain at larger q_{NN} , where for example contributions of nonnucleon intermediate states to the loop integral might be important, we assume that $F_{NN}(q_{NN}) = 1$ for $q_{NN} \geq q_0$.

In Fig. 4 we show the FSI effect on the total cross section for the reactions $pp \rightarrow ppa_0^0$ (upper part) and $pp \rightarrow pna_0^+$ (lower part) for $u(N)$, $s(N)$ and $t(f_1)$ channels. The solid lines show the calculation without FSI whereas the dashed lines indicate the results with

FSI. As seen from Fig. 4, the FSI effect is stronger for pn than for pp in the final state due to the Coulomb repulsive interaction in the pp system and the isospin dependence of the NN interaction at small relative momenta.

The results of our calculations for the total cross sections with FSI for the different isospin reactions are presented in Figs. 5, 6 as a function of $Q = \sqrt{s} - \sqrt{s_0}$. In Fig. 5 we show the total cross section for the pp reactions – $pp \rightarrow ppa_0^0$ (upper part) and $pp \rightarrow pna_0^+$ (lower part), whereas in Fig. 6 we display the results for the pn reactions – $pn \rightarrow ppa_0^-$ (upper part) and $pn \rightarrow pna_0^0$ (lower part). The solid lines with full dots and with open squares (r.h.s.) represent the results within the ρ_2 and (ρ_2, b_1) Regge exchange model. The short dotted lines (l.h.s.) corresponds to the $t(f_1)$ channel, the dotted lines to the $t(\eta)$ channel, the dashed lines to the $u(N)$ channel, the short dashed lines to the $s(N)$ channel. The dashed line in the right upper part of Fig. 5 is the incoherent sum of the contributions from $s(N)$ and $u(N)$ channels ($s + u$).

As seen from Figs. 5 and 6, the u - and s -channels give the dominant contribution; the $t(f_1)$ channel is small for all isospin reactions. For the reactions $pp \rightarrow pna_0^+$, $pn \rightarrow ppa_0^-$ and $pn \rightarrow pna_0^0$ the Regge exchange contribution (extended to low energies) becomes important and for the $pn \rightarrow pna_0^0$ reaction this contribution is even dominant near threshold. For the $pp \rightarrow ppa_0^0$ channel the Regge model predicts no contribution from ρ_2 and ρ_2, b_1 exchanges due to isospin arguments (i.e. the vertex with a coupling of three neutral components of isovectors vanishes); thus only s -, u - and $t(f_1)$ - channels are plotted in the upper part of Fig. 5.

Here we have to point out the influence of the interference between the s - and u -channels. According to the isospin coefficients from the OPE model presented in Table 1, the phase (of interference α) between the s - and u - channels $\mathcal{M}_{s(N)}^\pi + \exp(-i\alpha)\mathcal{M}_{u(N)}^\pi$ is equal to zero, i.e. the sign between $\mathcal{M}_{s(N)}^\pi$ and $\mathcal{M}_{u(N)}^\pi$ is 'plus'. The solid lines in Figs. 5, 6 indicate the coherent sum of $s(N)$ and $u(N)$ channels including the interference of the amplitudes ($s + u + int.$). One can see that for $pp \rightarrow pna_0^+$, $pn \rightarrow ppa_0^-$ and $pn \rightarrow pna_0^0$ reactions the interference is positive and increases the cross section, whereas for the $pp \rightarrow ppa_0^0$ channel the interference is strongly destructive since we have identical particles in the initial and final states and the contributions of s - and u -channels are very similar.

Here we would like to comment about an extension of the OPE (one-pion-exchange) model to an OBE (one-boson-exchange) approximation, i.e. accounting for the exchange of $\sigma, \rho, \omega, \dots$ mesons as well as for multi-meson exchanges. Generally speaking, the total cross section of a_0 production should contain the sum of all the contributions:

$$\sigma(NN \rightarrow NN a_0) = \sum_j \sigma_j,$$

where $j = \pi, \sigma, \rho, \omega, \dots$. Depending on their cut-off parameters the heavier meson exchanges might give a comparable contribution to the total cross section for a_0 production. An important point, however, is that near threshold (e.g. $Q \leq 0.3$ GeV) the energy behaviour of all those contributions is the same, i.e. it is proportional to the three-body phase space $\sigma_j \sim Q^2$ (when the FSI is switched off and the narrow

resonance width limit is taken). In this respect we can consider the one-pion exchange as an effective one and normalize it to the experimental cross section by choosing an appropriate value of Λ_π . The most appropriate choice for Λ_π is about $1\div 1.3$ GeV. Another question is related to the isospin of the effective exchange. As it is known from a series of papers on the reactions $NN \rightarrow NNX$, $X = \eta, \eta', \omega, \phi$ near threshold the most important contributions to the corresponding cross sections comes from π and ρ exchanges (see e.g. the review [41] and references therein). In line with those results we assume here that the dominant contribution to the cross section of the reaction $NN \rightarrow NN a_0$ comes also from the isovector exchanges (like π and ρ). In principle, it is also possible that some baryon resonances may contribute. However, as mentioned above, there is no information about resonances which couple to the $a_0 N$ system. Our assumptions thus enable us to make exploratory estimates of the a_0 production cross section without introducing free parameters that would be out of control by existing data. The model can be extended accordingly when new data on the a_0 production will be available.

Another important question is related to the choice of the form factor for a virtual nucleon, that – in line with the Bonn-Jülich potentials – we choose as given by (10), which corresponds to monopole form factors at the vertices. In the literature, furthermore, dipole-like form factors (at the vertices) are also often used (cf. Refs. [29, 30, 34, 35, 36]). However, there are no strict rules for the ‘correct’ power of the nucleon form factor. In physics terms, the actual choice of the power should not be relevant; we may have the same predictions for any reasonable choice of the power if the cut-off parameter Λ_N is fixed accordingly. Note, that Λ_N may also depend on the type of mesons involved at the vertices. Therefore, we can not simply employ the parameters from Refs. [29], [34] or others in case of the a_0 problem.

In our previous work [21] we have fixed Λ_N for the monopole related form factor (10) in the interval 1.2-1.3 GeV fitting the forward differential cross section of the reaction $pp \rightarrow da_0^+$ from [33]. On the other hand, the same data can be described rather well using a dipole form factor (at the vertices) with $\Lambda_N = 1.55$ -1.6 GeV (cf. Fig. 7). If we employ this dipole form factor with $\Lambda_N = 1.55$ -1.6 GeV in the present case we obtain practically identical predictions for the cross sections of the channels $pp \rightarrow pna_0^+$, $pn \rightarrow pna_0^0$, $pn \rightarrow ppa_0^-$, where the u -channel mechanism is dominant and $u - s$ interference is not too important. In the case of the channel $pp \rightarrow ppa_0^0$ we obtain cross sections by up to a factor of 2 larger for the dipole-like form factor in comparison to the monopole one. This is related to the strong destructive interference of the s and u exchange mechanisms, which slightly depends on the type of form factor used. However, our central result, that the cross section for the pna_0^+ final channel is about an order of magnitude higher than the ppa_0^0 channel in pp collisions, is robust (within less than a factor of 2) with respect to different choices of the form factor.

As seen from Figs. 5, 6, we get the largest cross section for the $pp \rightarrow pna_0^+$ isospin channel. For this reaction the u -channel gives the dominant contribution, the s -channel cross section is small such that the interference is not so essential as for the $pp \rightarrow ppa_0^0$

reaction.

The result within the Regge model is shown in Fig. 8 for the reactions $pp \rightarrow pna_0^+$, $pn \rightarrow pna_0^0$ (upper part) and $pn \rightarrow ppa_0^-$ (lower part) in a wide energy regime for $Q = 1 \text{ MeV} \div 10 \text{ GeV}$. The total cross section is calculated with the ρ_2 (dashed lines) and (ρ_2, b_1) (solid lines) Regge trajectories (with FSI) for a cut-off parameter $\Lambda_{\pi NN} = 1.05 \text{ GeV}$. In order to show the influence of the cut-off parameter $\Lambda_{\pi NN}$ in the Regge model we present in the lower part of Fig. 8 also the results for $\Lambda_{\pi NN} = 1.3 \text{ GeV}$ (dotted line for ρ_2 exchange and the dot-dashed line for the (ρ_2, b_1) trajectory). Changing the cut-off $\Lambda_{\pi NN}$ from 1.05 to 1.3 GeV gives a factor ~ 2 in the total cross section similar to the results within the effective Lagrangian model (cf. Fig. 3).

As it was already discussed in our previous study [21] an effective Lagrangian model cannot be extrapolated to high energies because it predicts the elementary amplitude $\pi N \rightarrow a_0 N$ to rise fast. Therefore, such model can only be employed not far from the threshold; at larger energies it has to be unitarized. On the other hand, the Regge model is valid at large energies and we have to worry, how close to the threshold we can extrapolate corresponding amplitudes. According to duality arguments one can expect that the Regge amplitude can be applied at low energy, too, if the reaction $\pi N \rightarrow a_0 N$ does not contain essential s -channel resonance contributions. In this case the Regge model might give a realistic estimate of the $\pi N \rightarrow a_0 N$ amplitude even near threshold.

Anyway, as we have shown in our previous paper [21] the Regge and u -channel model give quite similar results for the $\pi^- p \rightarrow a_0^0 n$ cross-section in the near threshold region; some differences in the cross sections of the reactions $NN \rightarrow NN a_0$ – as predicted by those two models – can be attributed to differences in the isospin factors and effects of NN antisymmetrization which is important near threshold (the latter was ignored in the Regge model formulated for larger energies).

5. The reaction $NN \rightarrow NN a_0 \rightarrow NN K \bar{K}$

5.1. The $K \bar{K}$ and $\pi\eta$ decay channels of the $a_0(980)$

The $a_0(980)$ meson production has not yet been measured in $NN \rightarrow NN a_0$ reactions. There are only a few $pp \rightarrow pp K \bar{K}$ and $pp \rightarrow pn K \bar{K}$ experimental data points. Therefore, it is important to analyse a possible resonance contribution to $K \bar{K}$ production in the reactions $NN \rightarrow NN X$, using the calculated $NN \rightarrow NN a_0$ amplitudes and the experimental fits obtained for the a_0 resonance mass distribution in the $K \bar{K}$ decay channel.

The amplitude for the $a_0(980)$ decays into $K \bar{K}$ and $\pi\eta$ modes can be parametrized by the well-known Flatté formula [42] which satisfies both requirements of analyticity and unitarity for the two-channels $\pi\eta$ and $K \bar{K}$.

In the case of the $a_0(980)$ resonance the mass distribution of the final $K \bar{K}$ system can be written as a product of the total cross section for a_0 production (with the 'running'

mass M) in the $NN \rightarrow NNa_0$ reaction (11) and the Flatté mass distribution function

$$\frac{d\sigma_{K\bar{K}}(s, M)}{dM^2} = \sigma_{a_0}(s, M) C_F \frac{M_R \Gamma_{a_0 K\bar{K}}(M)}{(M^2 - M_R^2)^2 + M_R^2 \Gamma_{tot}^2(M)} \quad (18)$$

with the total width $\Gamma_{tot}(M) = \Gamma_{a_0 K\bar{K}}(M) + \Gamma_{a_0 \pi\eta}(M)$. The partial widths

$$\begin{aligned} \Gamma_{a_0 K\bar{K}}(M) &= g_{a_0 K\bar{K}}^2 \frac{q_{K\bar{K}}}{8\pi M^2}, \\ \Gamma_{a_0 \pi\eta}(M) &= g_{a_0 \pi\eta}^2 \frac{q_{\pi\eta}}{8\pi M^2} \end{aligned} \quad (19)$$

are proportional to the decay momenta in the center-of-mass (in case of scalar mesons),

$$\begin{aligned} q_{K\bar{K}} &= \frac{[(M^2 - (m_K + m_{\bar{K}})^2)(M^2 - (m_K - m_{\bar{K}})^2)]^{1/2}}{2M} \\ q_{\pi\eta} &= \frac{[(M^2 - (m_\pi + m_\eta)^2)(M^2 - (m_\pi - m_\eta)^2)]^{1/2}}{2M} \end{aligned}$$

for a meson of mass M decaying to $K\bar{K}$ and $\pi\eta$, correspondingly. The branching ratios $Br(a_0 \rightarrow K\bar{K})$ and $Br(a_0 \rightarrow \pi\eta)$ are given by the integrals of the Flatté distribution over the invariant mass squared $dM^2 = 2M dM$:

$$Br(a_0 \rightarrow K\bar{K}) = \int_{m_K + m_{\bar{K}}}^{\infty} \frac{dM}{2M} \frac{C_F M_R \Gamma_{a_0 K\bar{K}}(M)}{(M^2 - M_R^2)^2 + M_R^2 \Gamma_{tot}^2(M)}, \quad (20)$$

$$\begin{aligned} Br(a_0 \rightarrow \pi\eta) &= \int_{m_K + m_{\bar{K}}}^{\infty} \frac{dM}{2M} \frac{C_F M_R \Gamma_{a_0 \pi\eta}(M)}{(M^2 - M_R^2)^2 + M_R^2 \Gamma_{tot}^2(M)} \\ &+ \int_{m_\pi + m_\eta}^{m_K + m_{\bar{K}}} \frac{dM}{2M} \frac{C_F M_R \Gamma_{a_0 \pi\eta}(M)}{(M^2 - M_R^2 - M_R \Gamma_{a_0 K\bar{K}}(M))^2 + M_R^2 \Gamma_{a_0 \pi\eta}^2(M)}. \end{aligned} \quad (21)$$

The parameters $C_F, g_{K\bar{K}}, g_{\pi\eta}$ have to be fixed under the constraint of the unitarity condition

$$Br(a_0 \rightarrow K\bar{K}) + Br(a_0 \rightarrow \pi\eta) = 1. \quad (22)$$

Choosing the parameter $\Gamma_0 = \Gamma_{a_0 \pi\eta}(M_R)$ in the interval $50 \div 100$ MeV as given by the PDG [43], one can fix the coupling $g_{\pi\eta}$ according to (19). In Ref. [45] a ratio of branching ratios has been reported,

$$r(a_0(980)) = \frac{Br(a_0 \rightarrow K\bar{K})}{Br(a_0 \rightarrow \pi\eta)} = 0.23 \pm 0.05, \quad (23)$$

for $m_{a_0} = 0.999$ GeV, which gives $Br(a_0 \rightarrow K\bar{K}) = 0.187$. In another recent study [44] the WA102 collaboration reported the branching ratio

$$\Gamma(a_0 \rightarrow K\bar{K})/\Gamma(a_0 \rightarrow \pi\eta) = 0.166 \pm 0.01 \pm 0.02, \quad (24)$$

which was determined from the measured branching ratio for the $f_1(1285)$ -meson. In our present analysis we use the results from [45], however, keeping in mind that this branching ratio $Br(a_0 \rightarrow K\bar{K})$ more likely gives an 'upper limit' for the $a_0 \rightarrow K\bar{K}$ decay.

Thus, the two other parameters in the Flatté distribution C_F and $g_{a_0 K \bar{K}}$ can be found by solving the system of integral equations, for example, Eq. (20) for $Br(a_0 \rightarrow K \bar{K}) = 0.187$ and the unitarity condition (22). For our calculations we choose either $\Gamma_{a_0 \pi \eta}(M_R) = 70$ MeV or 50 MeV, which gives two sets of independent parameters $C_F, g_{a_0 K \bar{K}}, g_{a_0 \pi \eta}$ for a fixed branching ratio $Br(a_0 \rightarrow K \bar{K}) = 0.187$:

$$\text{set 1 } (\Gamma_{a_0 \pi \eta} = 70 \text{ MeV}) : \quad (25)$$

$$g_{a_0 K \bar{K}} = 2.297, \quad g_{a_0 \pi \eta} = 2.189, \quad C_F = 0.365$$

$$\text{set 2 } (\Gamma_{a_0 \pi \eta} = 50 \text{ MeV}) : \quad (26)$$

$$g_{a_0 K \bar{K}} = 1.943, \quad g_{a_0 \pi \eta} = 1.937, \quad C_F = 0.354.$$

Note, that for the $K^+ K^-$ or $K^0 \bar{K}^0$ final state one has to take into account an isospin factor for the coupling constant, i.e. $g_{a_0 K^+ K^-} = g_{a_0 K^0 \bar{K}^0} = g_{a_0 K \bar{K}}/\sqrt{2}$, whereas $g_{a_0 K^+ \bar{K}^0} = g_{a_0 K^- \bar{K}^0} = g_{a_0 K \bar{K}}$.

5.2. Numerical results for the total cross section

In the upper part of Fig. 9 we display the calculated total cross section (within parameter *set 1*) for the reaction $pp \rightarrow pna_0^+ \rightarrow pnK^+ \bar{K}^0$ in comparison to the experimental data for $pp \rightarrow pnK^+ \bar{K}^0$ (solid dots) from Ref. [46] as a function of the excess energy $Q = \sqrt{s} - \sqrt{s_0}$. The dot-dashed and solid lines in Fig. 9 correspond to the coherent sum of $s(N)$ and $u(N)$ channels with interference ($s + u + int.$), calculated with a monopole form of the form factor (10) with $\Lambda_N = 1.24$ GeV and with a dipole form of (10) with $\Lambda_N = 1.35$ GeV, respectively. We mention that the latter (dipole) result is in better agreement with the constraints on the near-threshold production of a_0 in the reactions $\pi^- p \rightarrow K^- \bar{K}^0 p$ and $\pi^+ p \rightarrow K^+ \bar{K}^0 p$ [47]. In the middle part of Fig. 9 the solid lines with full dots and with open squares present the results within the ρ_2 and (ρ_2, b_1) Regge exchange model. The short dashed line shows the 4-body phase space (with constant interaction amplitude), while the dashed line is the parametrization from Sibirtsev et al. [48]. We note, that the cross sections for parameter *set 2* are similar to *set 1* and larger by a factor ~ 1.5 .

In the lower part of Fig. 9 we show the calculated total cross section (within parameter *set 1*) for the reaction $pp \rightarrow ppa_0^0 \rightarrow ppK^+ K^-$ as a function of $Q = \sqrt{s} - \sqrt{s_0}$ in comparison to the experimental data. The solid dots indicate the data for $pp \rightarrow ppK^0 \bar{K}^0$ from Ref. [46], the open square for $pp \rightarrow ppK^+ K^-$ is from the DISTO collaboration [49] and the full down triangles show the data from COSY-11 [50].

For the $pp \rightarrow ppa_0^0 \rightarrow ppK^+ K^-$ reaction (as for $pp \rightarrow ppa_0^0$) there is no contribution from meson Regge trajectories; s - and u -channels give similar contributions such that their interference according to the effective OPE model (line $s + u + int.$) is strongly destructive (cf. upper part of Fig. 5). The $t(f_1)$ contribution (short dotted line) is practically negligible, while the $t(\eta)$ -channel (dotted line) becomes important closer to the threshold.

Thus our model gives quite small cross sections for a_0^0 production in the $pp \rightarrow$

ppK^+K^- reaction which complicates its experimental observation for this isospin channel. The situation looks more promising for the $pp \rightarrow pna_0^+ \rightarrow pnK^+\bar{K}^0$ reaction since the a_0^+ production cross section is by an order of magnitude larger than the a_0^0 one. Moreover, as has been pointed out with respect to Fig. 5, the influence of the interference is not so strong as for the $pp \rightarrow ppa_0^0 \rightarrow ppK^+K^-$ reaction.

Here we stress again the limited applicability of the effective Lagrangian model (ELM) at high energies. As seen from the upper part of Fig. 9, the ELM calculations at high energies go through the experimental data, which is not realistic since also other channels contribute to $K^+\bar{K}^0$ production in pp reactions (cf. dashed line from Ref. [48]). Moreover, the ELM calculations are higher than the Regge model predictions which indicates, that the ELM amplitudes at high energies have to be reggeized or unitarized.

5.3. Numerical results for the invariant mass distribution

As follows from the lower part of Fig. 9, the a_0 contribution to the K^+K^- production in the $pp \rightarrow ppK^+K^-$ reaction near the threshold is hardly seen. With increasing energy the cross section grows up, however, even at $Q = 0.111$ GeV the full cross section with interference ($s + u + int.$) gives only a few percent contribution to the $0.11 \pm 0.009 \pm 0.046$ μb 'nonresonant' cross section (without $\phi \rightarrow K^+K^-$) from the DISTO collaboration [49].

To clarify the situation with the relative contribution of a_0^0 to the total K^+K^- production in pp reactions we calculate the K^+K^- invariant mass distribution for the $pp \rightarrow ppK^+K^-$ reaction at $p_{lab} = 3.67$ GeV/ c , which corresponds to the kinematical conditions for the DISTO experiment [49]. The differential results are presented in Fig. 10. The upper part shows the calculation within parameter *set 1*, whereas the lower part corresponds to *set 2*. The dot-dashed lines (lowest curves) indicate the coherent sum of $s(N)$ and $u(N)$ channels with interference ($s + u + int.$) for the a_0 contribution. However, one has to consider also the contribution from the f_0 scalar meson, i.e. the $pp \rightarrow pp f_0 \rightarrow ppK^+K^-$ reaction. The f_0 production in pp reactions has been studied in detail in Ref. [51]. Here we use the result from this previous work [51] and show in Fig. 10 the contribution from the f_0 meson calculated with parameter *set A* from Ref. [51] as the solid line with open circles (f_0).

We find that when adding the f_0 contribution to the phase-space of nonresonant K^+K^- production (the short dotted lines in Fig. 10) and the contribution from ϕ decays (resonance peak around 1.02 GeV), the sum (solid) lines almost perfectly describe the DISTO data. This means that there is no visible signal for an a_0^0 contribution in the DISTO data according to our calculations while the f_0 meson gives some contribution to the K^+K^- invariant mass distribution at low invariant masses M , that is $\sim 12\%$ of the total 'nonresonant' cross section from the DISTO collaboration [49]. Thus the reaction $pp \rightarrow pnK^+\bar{K}^0$ is more promising for a_0 measurements as it has been pointed out in the previous subsection.

For an experimental determination of the a_0^+ we present the invariant mass

distribution of $K^+\bar{K}^0$ in the reaction $pp \rightarrow pnK^+\bar{K}^0$ at different Q (solid lines) in Fig. 11. The dashed lines show the invariant mass distributions for 'background' (i.e. according to phase space with constant interaction amplitude) under the assumption that the integrals below the solid and dashed lines are the same for each Q . We see that the shape of the solid and dashed lines are practically the same for $Q \leq 50$ MeV. Noticeable differences between the lines can be found for $Q \geq 100$ MeV. This means that a separation of the resonance contribution from the background very close to threshold can be done only in the case when the background is small or very well known.

6. Conclusions

In this work we have estimated the cross sections of a_0 production in the reactions $pp \rightarrow ppa_0^0$, $pp \rightarrow pna_0^+$, $pn \rightarrow ppa_0^-$ and $pn \rightarrow pna_0^0$ near threshold and at medium energies. Using an effective Lagrangian approach with one-pion exchange we have analyzed different contributions to the cross section corresponding to t -channel diagrams with $\eta(550)$ - and $f_1(1285)$ -meson exchanges as well as s and u -channel graphs with an intermediate nucleon. We use the same parameters as in our previous paper where we describe rather well the Berkeley data [33] on the reaction $pp \rightarrow da_0^+$.

We additionally have considered the t -channel Reggeon exchange mechanism with parameters normalized to the Brookhaven data for $\pi^-p \rightarrow a_0^-p$ at 18 GeV/c [39]. These results have been used to calculate the contribution of a_0 mesons to the cross sections of the reactions $pp \rightarrow pnK^+\bar{K}^0$ and $pp \rightarrow ppK^+K^-$. Due to unfavourable isospin Clebsh-Gordan coefficients as well as rather strong destructive interference of the s - and u -channel contributions our model gives quite small cross sections for a_0^0 production in the $pp \rightarrow ppK^+K^-$ reaction. However, the a_0^+ production cross section in the $pp \rightarrow pna_0^+ \rightarrow pnK^+\bar{K}^0$ reaction should be larger by about an order of magnitude. Therefore the experimental observation of a_0^+ in the reaction $pp \rightarrow pnK^+\bar{K}^0$ is much more promising than the observation of a_0^0 in the reaction $pp \rightarrow ppK^+K^-$. We note in passing that the $\pi\eta$ decay channel is experimentally more challenging since, due to the larger nonresonant background [52], the identification of the η -meson (via its decay into photons) in a neutral-particle detector is required.

We have also analyzed invariant mass distributions of the $K\bar{K}$ system in the reaction $pp \rightarrow pNa_0 \rightarrow pNK\bar{K}$ at different excess energies Q not far from threshold. Our analysis of the DISTO data on the reaction $pp \rightarrow ppK^+K^-$ at 3.67 GeV/c has shown that the a_0^0 -meson is practically not seen in $d\sigma/dM$ at low invariant masses, however, the f_0 -meson gives some visible contribution. In this respect the possibility to measure the a_0^+ meson in $d\sigma/dM$ for the reaction $pp \rightarrow pnK^+\bar{K}^0$ (or $\rightarrow dK^+\bar{K}^0$) looks much more promising not only due to a much larger contribution for the a_0^+ , but also due to the absence of the f_0 meson in this channel.

Experimental data on a_0 production in NN collisions are practically absent (except of the a_0 observation in the reaction $pp \rightarrow dX$ [33]). Such measurements might give new information on the a_0 structure. According to Atkinson et al. [53] a relatively strong

production of the a_0 (the same as for the $b_1(1235)$) in non-diffractive reactions can be considered as evidence for a $q\bar{q}$ state rather than a $qq\bar{q}\bar{q}$ state. For example the cross section of a_0 production in γp reactions at 25–50 GeV is about 1/6 of the cross sections for ρ and ω production. Similar ratios are found in the two-body reaction $pp \rightarrow dX$ at 3.8–6.3 GeV/c where $\sigma(pp \rightarrow da_0^+) = (1/4 \div 1/6)\sigma(pp \rightarrow d\rho^+)$.

In our case we can compare a_0 and ω production. Our model predicts $\sigma(pp \rightarrow pna_0^+) = 30 \div 70\mu\text{b}$ at $Q \simeq 1$ GeV (see Fig. 8) which can be compared with $\sigma(pp \rightarrow pp\omega) \simeq 100 - 200\mu\text{b}$ at the same Q . If such a large cross section could be detected this would be a serious argument in favour of the $q\bar{q}$ model for the a_0 .

To distinguish between the threshold cusp scenario and a resonance model one can exploit different analytical properties of the a_0 production amplitudes in those approaches. In case of a genuine resonance the amplitude of $\eta\pi$ and $K\bar{K}$ production through the a_0 has a pole and satisfies the factorization property. This implies that the shapes of the invariant mass distributions in the $\eta\pi$ and $K\bar{K}$ channels should not depend on the specific reaction in which the a_0 resonance is produced (for $Q \geq \Gamma_{tot}$). On the other hand, for the threshold cusp scenario the a_0 bump is produced through the $\pi\eta$ final state interaction. The corresponding amplitude has a square root singularity and in general can not be factorized (see e.g. Ref. [40] where the factorization property was disproven for pp FSI in the reaction $pp \rightarrow ppM$). This implies that for a threshold bump the invariant mass distributions in the $\eta\pi$ and $K\bar{K}$ channels are expected to be different for different reactions and will even depend on kinematical conditions (i.e. initial energy and momentum transfer) at the same excess energy, e.g. $Q \simeq 1$ GeV.

6.1. Acknowledgments

The authors are grateful to J. Ritman for stimulating discussions and useful suggestions, to V. Baru for providing the parametrization of the FSI enhancement factor and to V. Kleber for a careful reading of the manuscript.

References

- [1] Brown G E and Rho M 2002 *Phys. Rep.* **363** 85
- [2] Cassing W and Bratkovskaya E L 1999 *Phys. Rep.* **308** 65
- [3] Rapp R and Wambach J 2000 *Adv. Nucl. Phys.* **25** 1
- [4] Close F E *et al.* 1993 *Phys. Lett.* **B319** 291
- [5] Genovese M *et al.* 1994 *Nuovo Cim.* **A107** 1249
- [6] Janssen G *et al.* 1995 *Phys. Rev. D* **52** 2690
- [7] Anisovich V V *et al.* 1995 *Phys. Lett. B* **355** 363
- [8] Törnqvist N A 1982 *Phys. Rev. Lett.* **49** 624
- [9] Maltman K, ‘Scalar Meson Decay Constants and the Nature of the $a_0(980)$ ’, *Review talk at Hadron-99, Beijing, Aug. 24–28, 1999*; hep-ph/0005155; 2000 *Nucl. Phys. A* **675** 209
- [10] Narison S, ‘Gluonic Scalar Mesons Hybrids from QCD Spectral Sum Rules’, *Review talk at Hadron-99, Beijing, Aug. 24–28, 1999*; hep-ph/9909470; 2000 *Nucl. Phys. Proc. Suppl.* **86** 242
- [11] Montanet L 2000 *Nucl. Phys. B (Proc. Suppl.)* **86** 381

- [12] Anisovich V V, Montanet L and Nikonov V N 2000 *Phys. Lett. B* **480** 19
- [13] Narison S 2001 *Nucl.Phys. Proc. Suppl.* **96** 244
- [14] Achasov N N, Devyanin S A and Shestakov G N 1979 *Phys. Lett. B* **88** 367
- [15] Achasov N N and Shestakov G N 1997 *Phys. Rev. D* **56** 212
- [16] Barnes T 1985 *Phys. Lett. B* **165** 434
- [17] Krehl O, Rapp R and Speth J 1997 *Phys. Lett. B* **390** 23
- [18] Kerbikov B O and Tabakin F 2000 *Phys. Rev. C* **62** 064601
- [19] Close F E and Kirk A 2000 *Phys. Lett. B* **489** 24
- [20] Grishina V Yu *et al.* 2001 *Phys. Lett. B* **521** 217
- [21] Grishina V Yu *et al.* 2000 *Eur. Phys. J. A* **9** 277
- [22] Chernyshev V *et al.*, COSY proposal #55 ‘Study of a_0^+ mesons at ANKE’ (1997) *available via www: <http://ikpd15.ikp.kfa-juelich.de:8085/doc/Anke.html>*; Kondratyuk L A *et al. Preprint ITEP 18-97*, Moscow (1997).
- [23] Büscher M *et al.*, Beam-time request for COSY proposal #55 ‘Study of a_0^+ mesons at ANKE’ (2000) *available via www: <http://ikpd15.ikp.kfa-juelich.de:8085/doc/Anke.html>*.
- [24] Büscher M *et al.*, Status report for COSY experiment #55 ‘Study of a_0^+ mesons at ANKE’ and Proposal ‘Investigation of neutral scalar mesons a_0^0/f_0 with ANKE’ *available via www: <http://ikpd15.ikp.kfa-juelich.de:8085/doc/Anke.html>*.
- [25] Machleidt R, Holinde K and Elster Ch 1987 *Phys. Rep.* **149** 1
- [26] Hippchen T *et al.* 1991 *Phys. Rev. C* **44** 1323; Mull V *et al.* 1991 *Phys. Rev. C* **44** 1337
- [27] Mull V and Holinde K 1995 *Phys. Rev. C* **51** 2360
- [28] Chung W S, Li G Q and Ko C M 1997 *Nucl. Phys. A* **625** 371
- [29] Nakayama K *et al.* 1998 *Phys. Rev. C* **57** 1580
- [30] Feuster T and Mosel U 1998 *Phys. Rev. C* **58** 457; 1999 *C* **59** 460.
- [31] Smith G A 1987 *The elementary structure of Matter* Les Houches, p. 197.
- [32] Amsler C *et al.* 1993 *Z. Phys. C* **58** 175
- [33] Abolins M A *et al.* 1970 *Phys. Rev. Lett.* **25** 469
- [34] Pearce B C and Jennings B K 1991 *Nucl. Phys. A* **528** 655
- [35] Haberzettl H *et al.* 1998 *Phys. Rev. C* **58** R40
- [36] Nakayama K *et al.* 2000 *Phys. Rev. C* **60** 055209
- [37] Titov A I, Kämpfer B and Reznik B L 2000 *Eur. Phys. A* **7** 543
- [38] Baru V *et al.* 2000 *Preprint ITEP 30-00*, Moscow
- [39] Dzierba A R. *Proceedings of the Second Workshop on Physics and Detectors for DAΦNE’95, Frascati, 1995*, edited by R. Baldini *et al.*, 1996 Frascati Physics Series **4** 99
- [40] Baru V *et al.* nucl-th/0006075, 2001 *Phys. Atom. Nucl.* **64** 579
- [41] Nakayama K nucl-th/0108032.
- [42] Flatté S 1976 *Phys. Lett. B* **63** 224
- [43] Caso C *et al. (Particle Data Group)* 2000 *Eur. Phys. J. C* **15** 1
- [44] Barberis D *et al. (WA102 Collaboration)* 1998 *Phys. Lett. B* **440** 225
- [45] Adomeit J *et al.* 1998 *Phys. Rev. D* **57** 3860
- [46] Landolt-Börnstein 1988 *New Series*, ed. H. Schopper, I/12
- [47] Kondratyuk *et al.* 2002 submitted to *Phys. Atom. Nucl.*
- [48] Sibirtsev A A, Cassing W and Ko C M 1997 *Z. Phys. A* **358** 101
- [49] Balestra F *et al.* 2001 *Phys. Rev. C* **63** 024004
- [50] Quentmeier C *et al.* 2001 *Phys. Lett. B* **515** 276
- [51] Bratkovskaya E L *et al.* 1999 *Eur. Phys. J. A* **4** 165
- [52] Müller H 2001 *Eur. Phys. J. A* **11** 113
- [53] Atkinson M *et al.* 1984 *Phys. Lett. B* **B 138** 459

Reaction j (mechanism α)	$\xi_{j(\alpha)}^\pi[ab; cd]$	$\xi_{j(\alpha)}^\pi[ab; dc]$	$\xi_{j(\alpha)}^\pi[ba; dc]$	$\xi_{j(\alpha)}^\pi[ba; cd]$
$pp \rightarrow ppa_0^0$ ($t(\eta), t(f_1)$)	$+1/\sqrt{2}$	$-1/\sqrt{2}$	$+1/\sqrt{2}$	$-1/\sqrt{2}$
($s(N)$)	$+1/\sqrt{2}$	$-1/\sqrt{2}$	$+1/\sqrt{2}$	$-1/\sqrt{2}$
($u(N)$)	$+1/\sqrt{2}$	$-1/\sqrt{2}$	$+1/\sqrt{2}$	$-1/\sqrt{2}$
Regge	0	0	0	0
$pp \rightarrow pna_0^+$ ($t(\eta), t(f_1)$)	$-\sqrt{2}$	0	0	$+\sqrt{2}$
($s(N)$)	0	$+\sqrt{2}$	$-\sqrt{2}$	0
($u(N)$)	$+2\sqrt{2}$	$-\sqrt{2}$	$+\sqrt{2}$	$-2\sqrt{2}$
Regge	-1	+1	-1	+1
$pn \rightarrow ppa_0^-$ ($t(\eta), t(f_1)$)	+1	-1	0	0
($s(N)$)	-2	+2	-1	+1
($u(N)$)	0	0	+1	-1
Regge	$+1/\sqrt{2}$	$-1/\sqrt{2}$	$-1/\sqrt{2}$	$+1/\sqrt{2}$
$pn \rightarrow pna_0^0$ ($t(\eta), t(f_1)$)	-1	0	+1	0
($s(N)$)	-1	-2	+1	+2
($u(N)$)	-1	+2	+1	-2
Regge	0	$+\sqrt{2}$	0	$-\sqrt{2}$

Table 1. Coefficients in Eq. (1) for different mechanisms of the $pp \rightarrow ppa_0^0$, $pp \rightarrow ppa_0^+$, $pn \rightarrow ppa_0^-$ and $pn \rightarrow pna_0^0$ reactions.

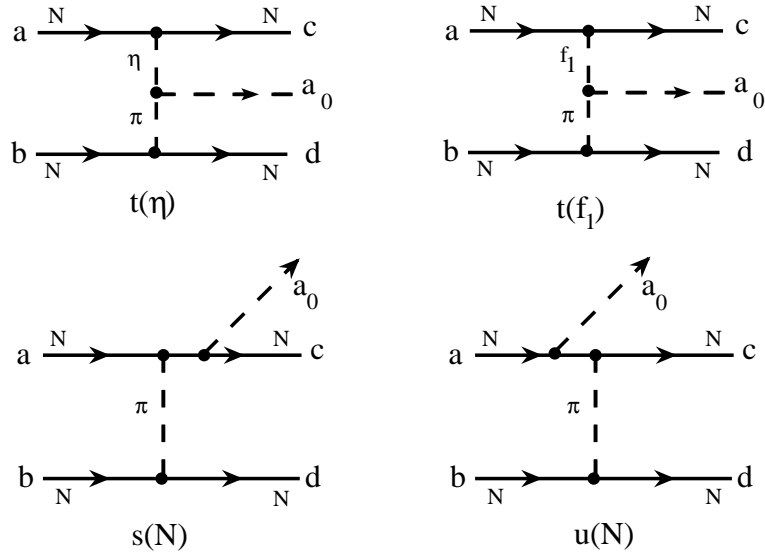


Figure 1. Diagrams for a_0 production in the reaction $NN \rightarrow a_0NN$ near threshold as considered in the present study.

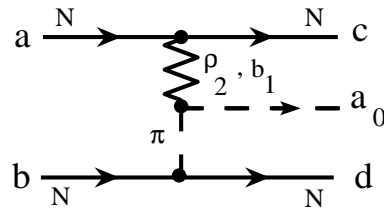


Figure 2. The diagram for a_0 production in the reaction $NN \rightarrow NN a_0$ within the Regge exchange model.

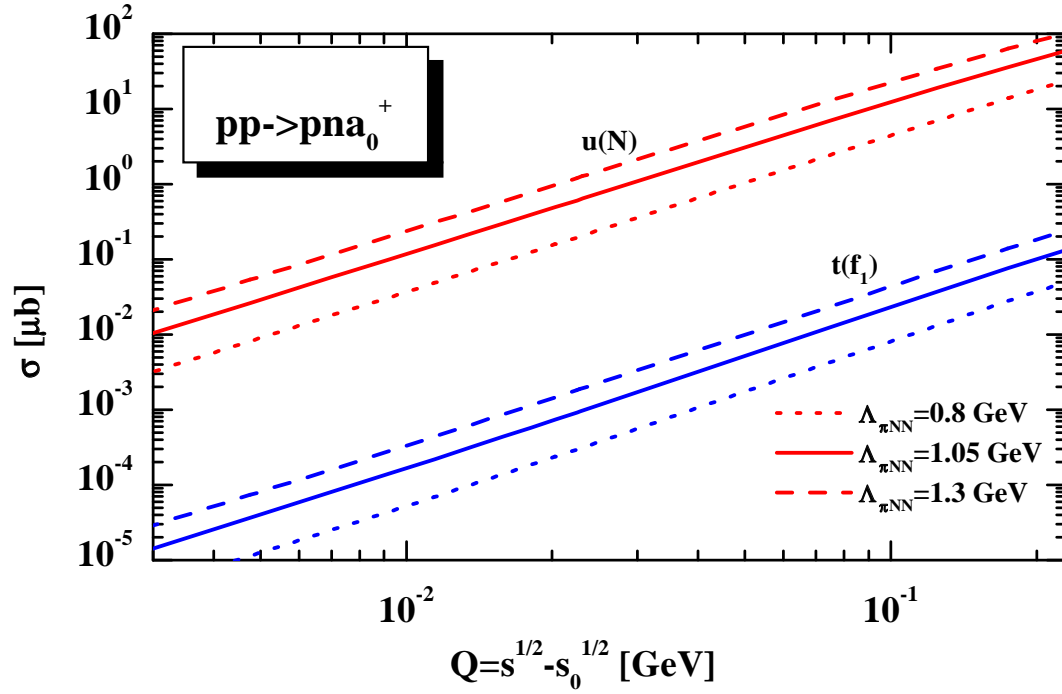


Figure 3. The total cross section for the reaction $pp \rightarrow pna_0^+$ for $u(N)$ and $t(f_1)$ channels as a function of the excess energy $Q = \sqrt{s} - \sqrt{s_0}$ for different cut-off parameters $\Lambda_{\pi NN} = 0.8$ GeV (dotted lines), $\Lambda_{\pi NN} = 1.05$ GeV (solid lines) and $\Lambda_{\pi NN} = 1.3$ GeV (dashed lines).

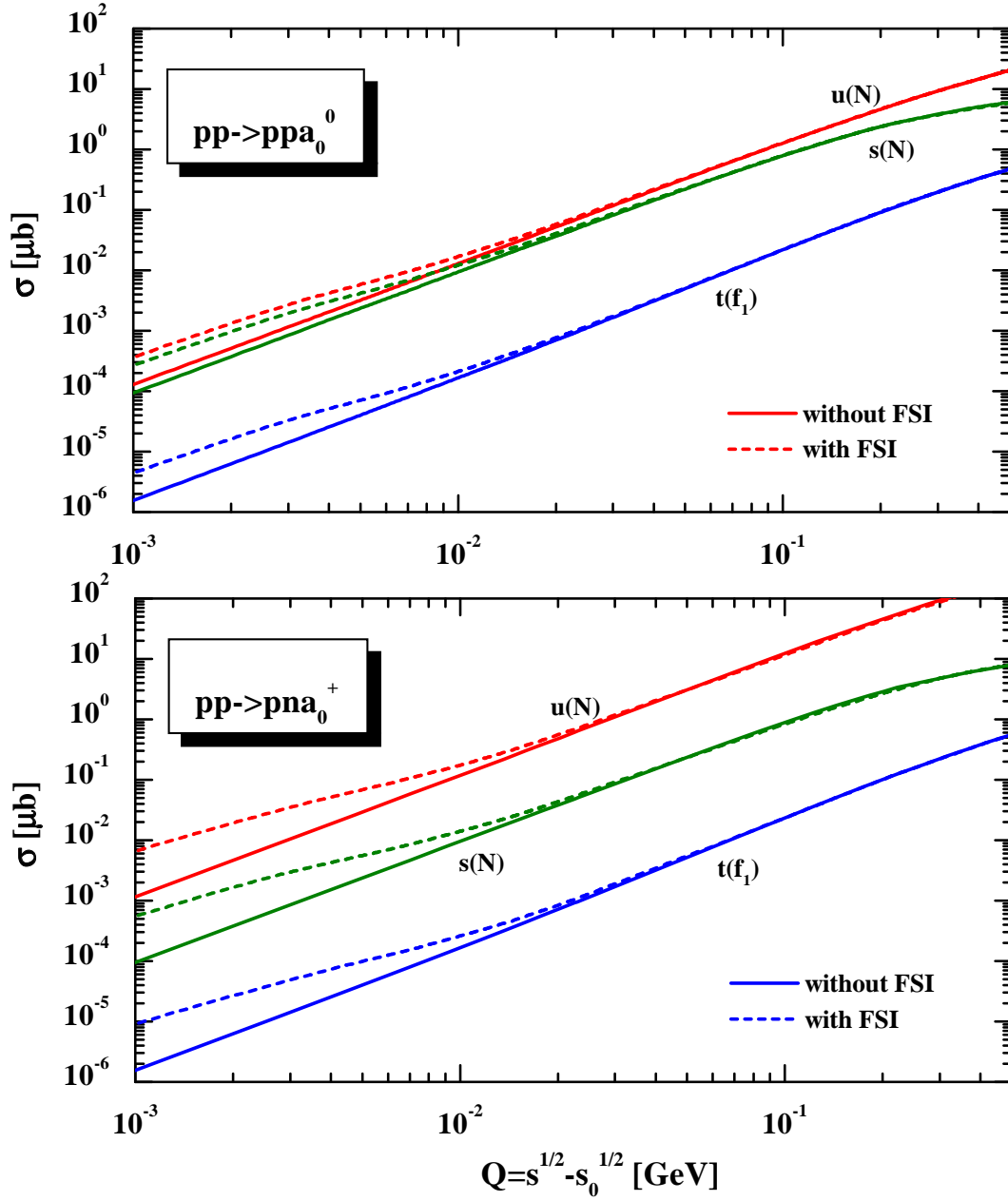


Figure 4. The total cross section for the reactions $pp \rightarrow ppa_0^0$ (upper part) and $pp \rightarrow pna_0^+$ (lower part) as a function of the excess energy $Q = \sqrt{s} - \sqrt{s_0}$ for $u(N)$, $s(N)$ and $t(f_1)$ channels calculated without FSI (solid lines) and with FSI (dashed lines).

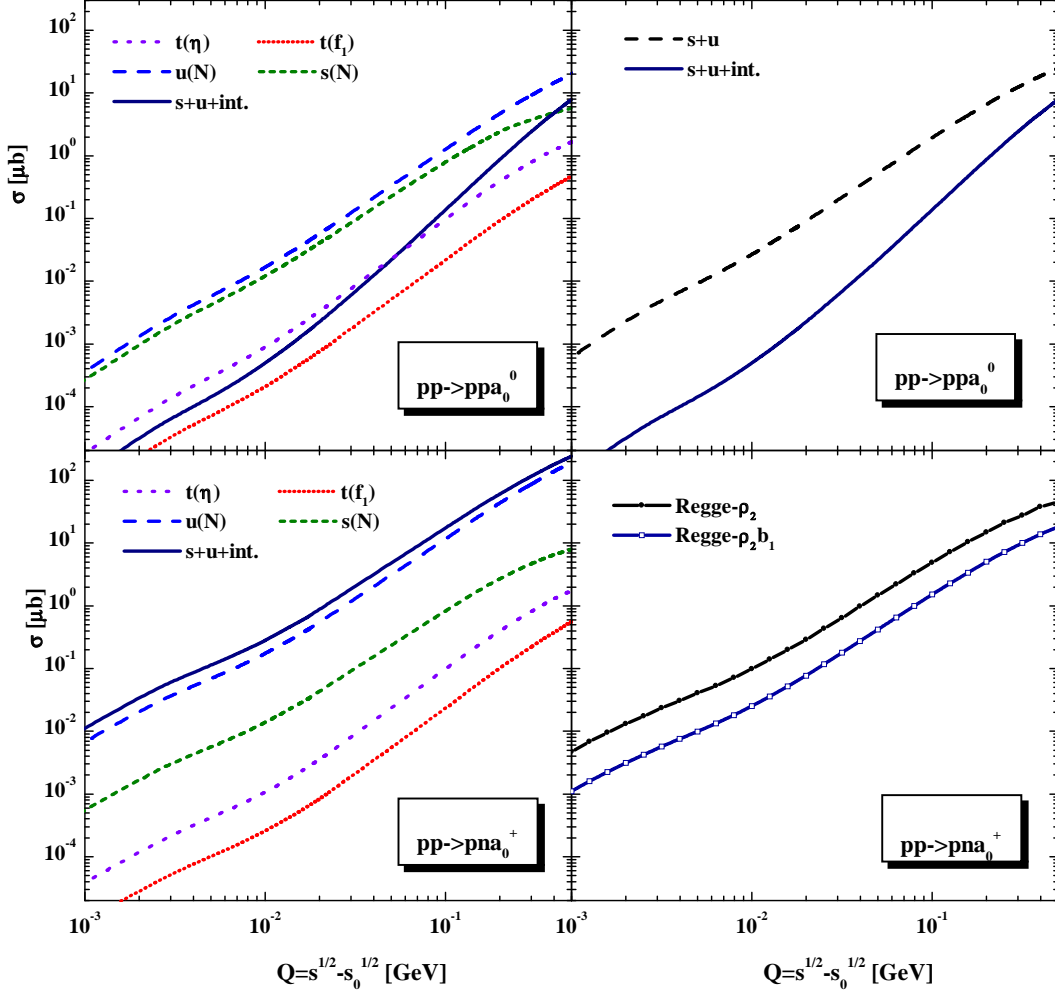


Figure 5. The total cross sections for the reactions $pp \rightarrow ppa_0^0$ (upper part) and $pp \rightarrow pna_0^+$ (lower part) as a function of the excess energy $Q = \sqrt{s} - \sqrt{s_0}$ calculated with FSI. The short dotted lines (l.h.s.) corresponds to the $t(f_1)$ channel, the dotted lines to the $t(\eta)$ channel, the dashed lines to the $u(N)$ channel, the short dashed lines to the $s(N)$ channel. The dashed line (upper part, r.h.s.) is the incoherent sum of the contributions from $s(N)$ and $u(N)$ channels ($s + u$). The solid lines indicate the coherent sum of $s(N)$ and $u(N)$ channels with interference ($s + u + int.$). The solid lines with full dots and with open squares (lower part, r.h.s.) present the results within the ρ_2 and (ρ_2, b_1) Regge exchange model.

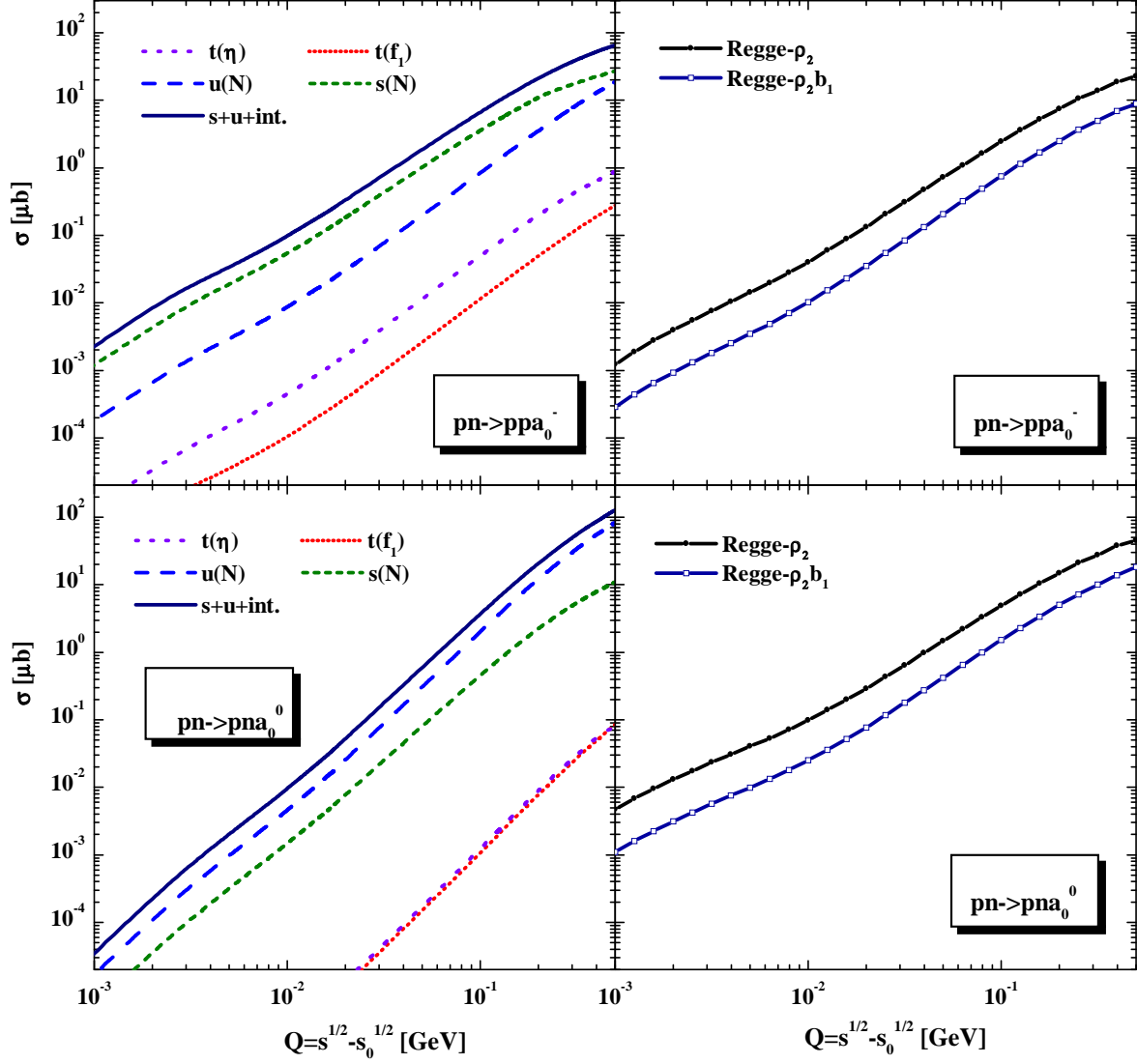


Figure 6. The total cross sections for the reactions $pn \rightarrow ppa_0^-$ (upper part) and $pn \rightarrow pna_0^0$ (lower part) as a function of $Q = \sqrt{s} - \sqrt{s_0}$ calculated with FSI. The assignment of the individual lines is the same as in Fig. 5. The results from the effective OPE model are shown on the l.h.s. while those from the ρ_2 and $\rho_2 b_1$ Regge approach are displayed on the r.h.s.

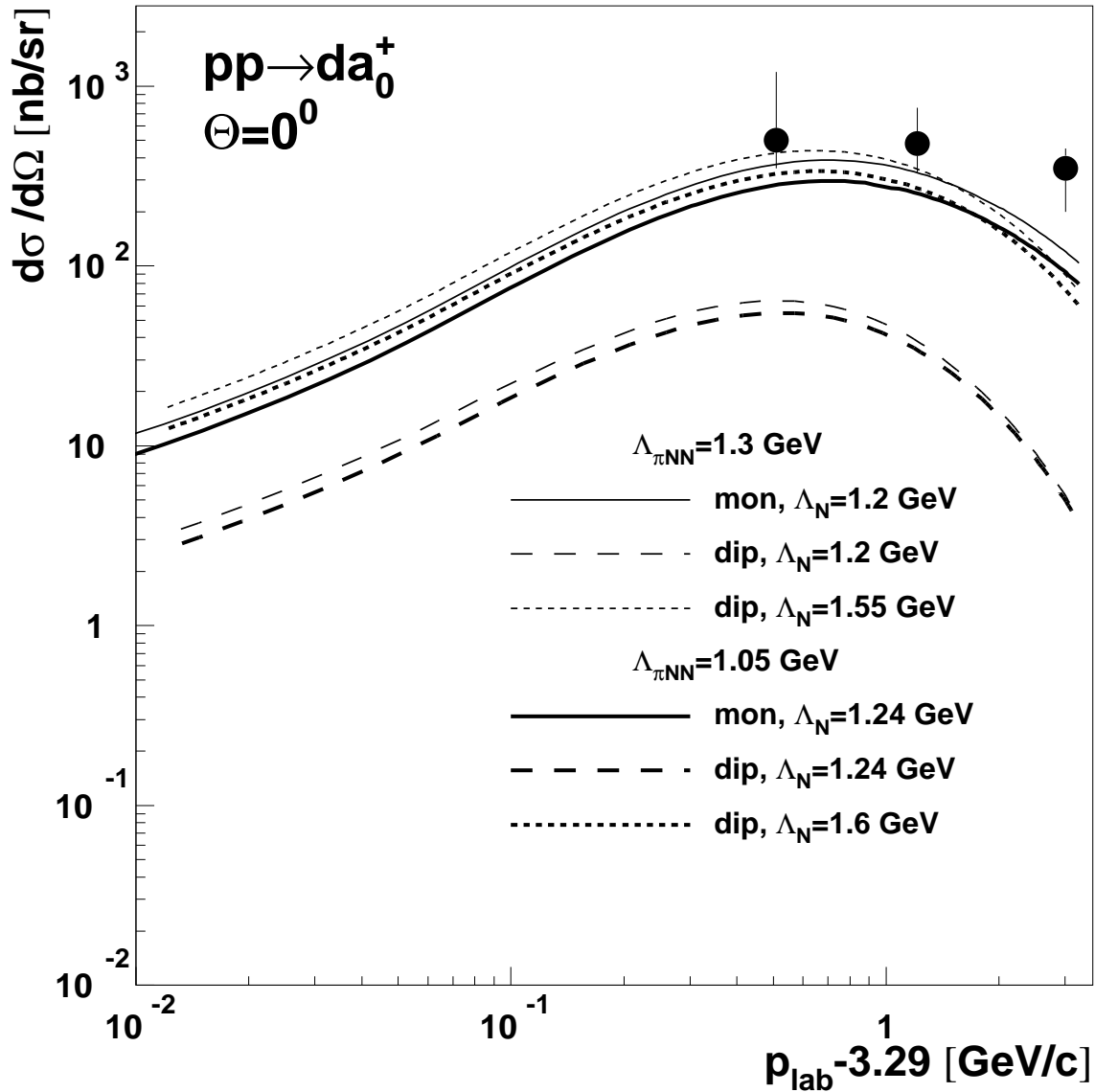


Figure 7. Forward differential cross section of the reaction $pp \rightarrow da_0^+$ as a function of $(p_{\text{lab}} - 3.29) \text{ GeV/c}$. The bold and thin solid curves are calculated at $\Lambda_{\pi NN} = 1.05$ and 1.3 GeV , respectively. The solid curves correspond to a monopole nucleon form factor with $\Lambda_N = 1.2$ (thin) and 1.24 GeV (bold). The long-dashed and short-dashed curves are calculated using the dipole nucleon form factor for different values of Λ_N as shown in the figure. The experimental data are taken from Ref. [33].

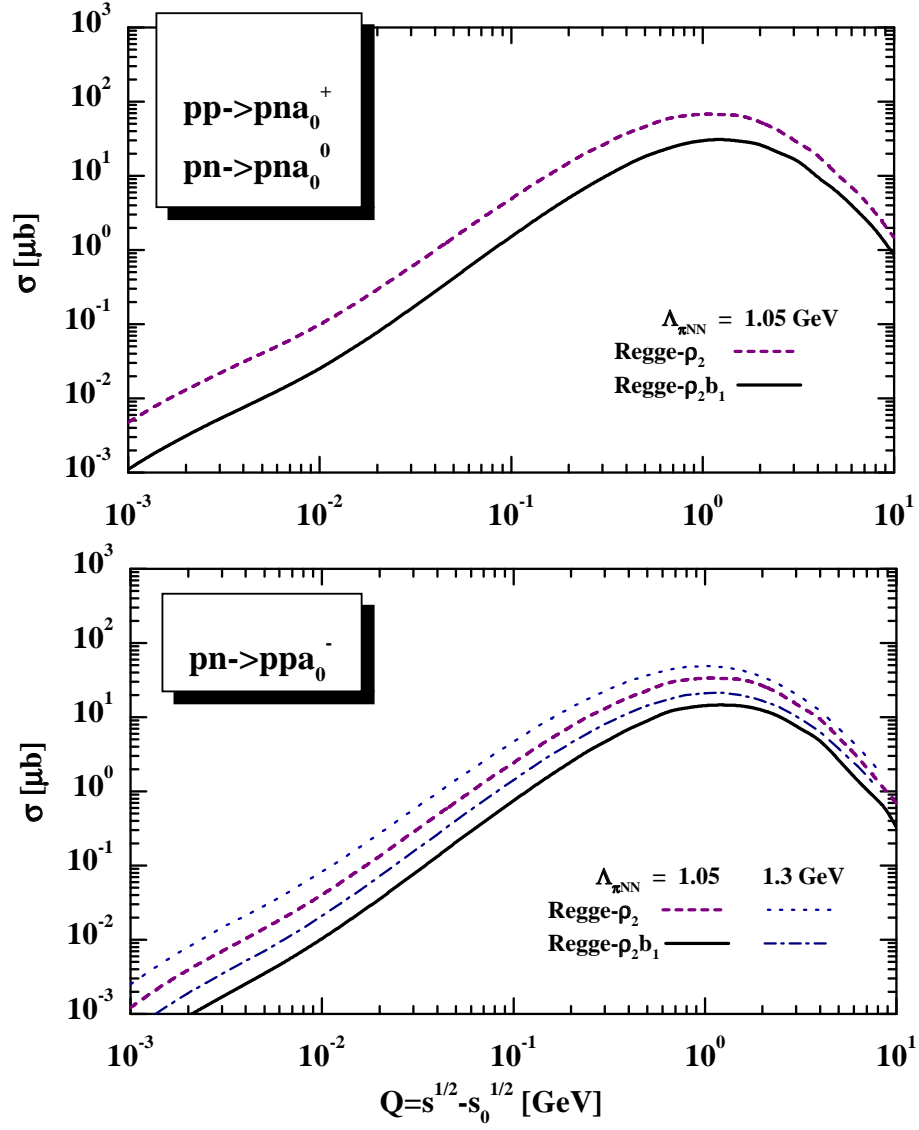


Figure 8. The total cross sections for the reactions $pp \rightarrow pna_0^+$, $pn \rightarrow pna_0^0$ (upper part) and $pn \rightarrow ppa_0^-$ (lower part) as a function of $Q = \sqrt{s} - \sqrt{s_0}$ calculated within the ρ_2 (dashed lines) and (ρ_2, b_1) (solid lines) Regge exchange model (with FSI) for cut-off parameters $\Lambda_{\pi NN} = 1.05$ GeV. The dotted and dot-dashed lines in the lower part show the results for $\Lambda_{\pi NN} = 1.3$ GeV within the ρ_2 and (ρ_2, b_1) exchanges, respectively.

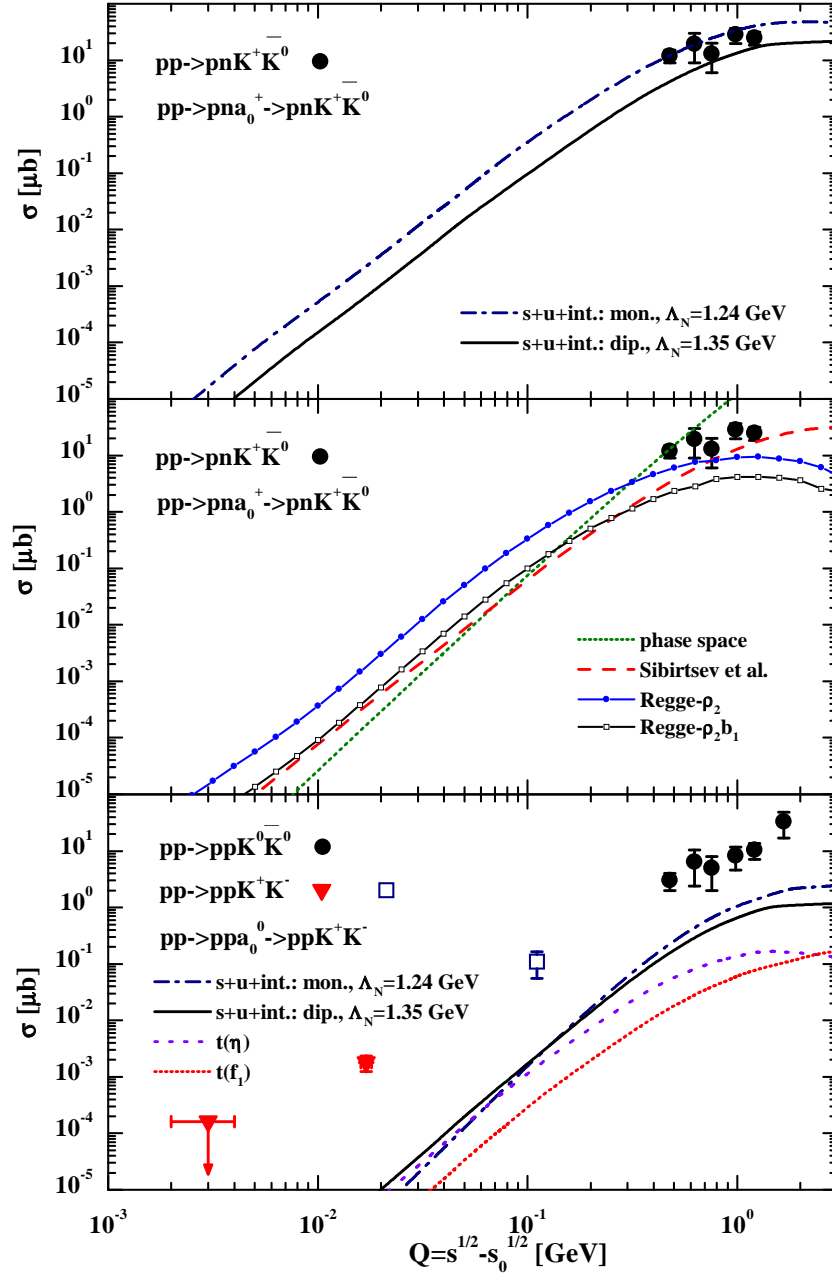


Figure 9. Upper part: the calculated total cross section (within parameter *set 1*) for the reaction $pp \rightarrow pna_0^+ \rightarrow pnK^+\bar{K}_0$ in comparison to the experimental data for $pp \rightarrow pnK^+\bar{K}_0$ (solid dots) from Ref. [46] as a function of $Q = \sqrt{s} - \sqrt{s_0}$. The dot-dashed and solid lines correspond to the coherent sum of $s(N)$ and $u(N)$ channels with interference ($s + u + int.$) calculated with a monopole form of the form factor (10) with $\Lambda_N = 1.24$ GeV and with a dipole form of (10) with $\Lambda_N = 1.35$ GeV, respectively. Middle part: the solid lines with full dots and with open squares represent the results within the ρ_2 and (ρ_2, b_1) Regge exchange model. The short dashed line shows the 4-body phase space (with constant interaction amplitude); the dashed line is the parametrization from Sibirtsev et al. [48]. Lower part: the calculated total cross section (within parameter *set 1*) for the reaction $pp \rightarrow ppa_0^0 \rightarrow ppK^+K^-$ as a function of $Q = \sqrt{s} - \sqrt{s_0}$ in comparison to the experimental data. The solid dots indicate the data for $pp \rightarrow ppK_0\bar{K}_0$ from Ref. [46], the open square for $pp \rightarrow ppK^+K^-$ from Ref. [49]; the full down triangles show the data from Ref. [50].

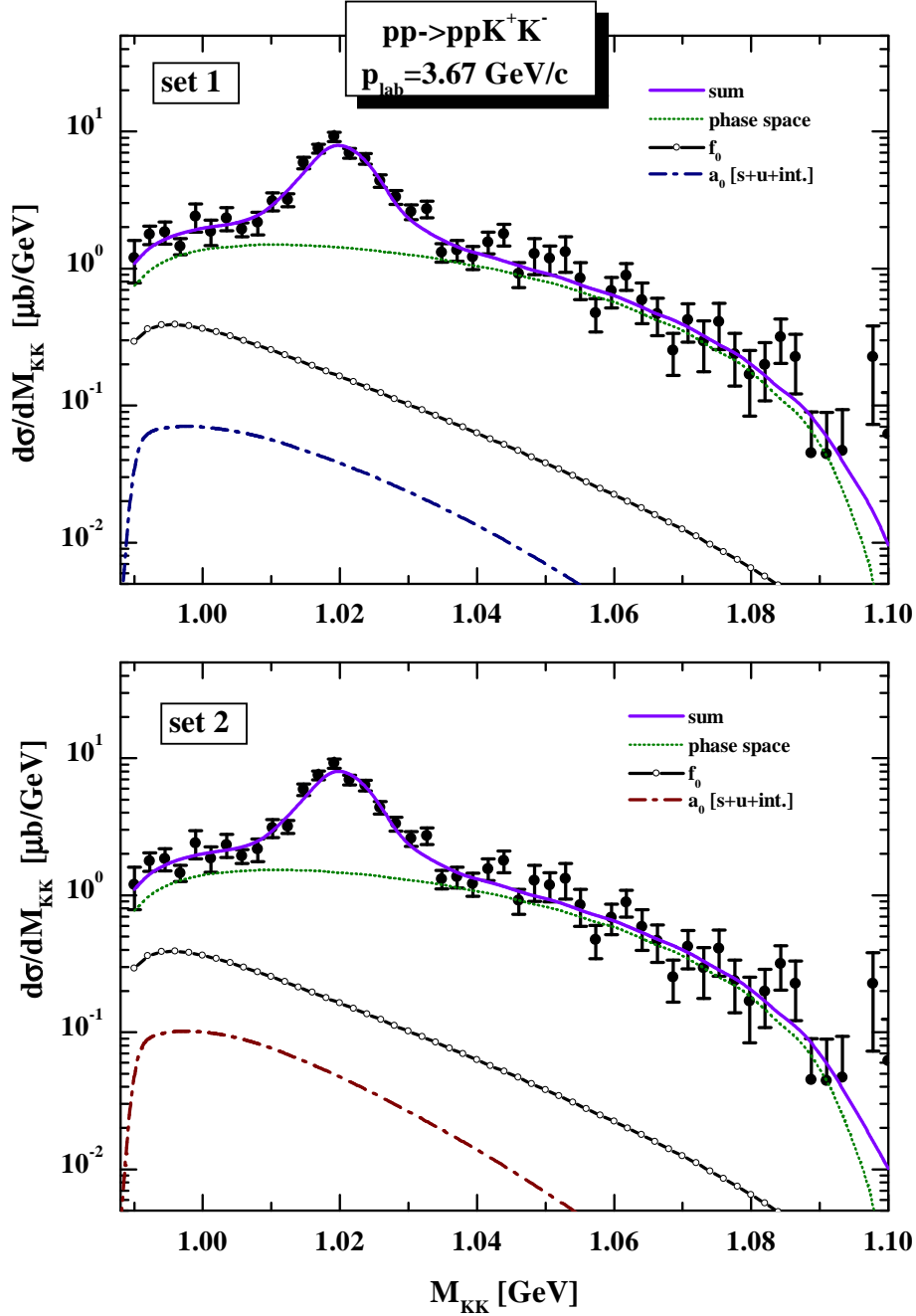


Figure 10. The K^+K^- invariant mass distribution for the $pp \rightarrow ppK^+K^-$ reaction at $p_{lab} = 3.67$ GeV/c. The short dotted lines indicate the 4-body phase space with constant interaction amplitude, the dot-dashed lines show the coherent sum of $s(N)$ and $u(N)$ channels with interference ($s + u + int.$). The solid lines with open circles correspond to the f_0 contribution from Ref. [51]. The thick solid lines show the sum of all contributions including the decay $\phi \rightarrow K^+K^-$. The experimental data are taken from Ref. [49].

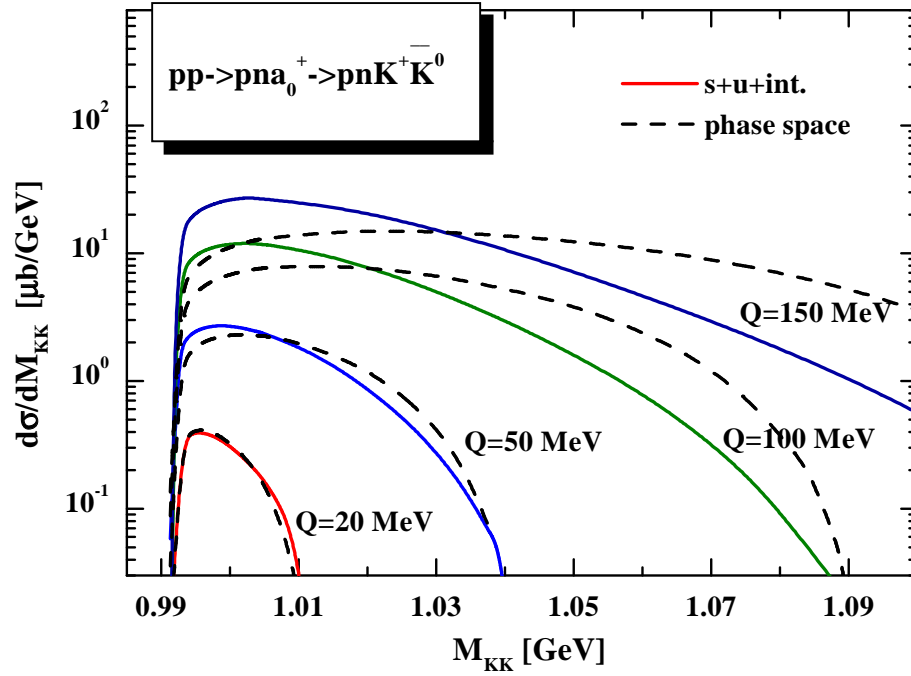


Figure 11. The $K^+\bar{K}^0$ invariant mass distribution for the $pp \rightarrow pnK^+\bar{K}^0$ reaction at different $Q = \sqrt{s} - \sqrt{s_0}$. The solid lines describe the a_0^+ resonance contributions. The dashed lines show the invariant mass distributions for 'background' under the assumption that the integrals below the solid and dashed lines are the same for each Q .